Gas-Kinetic Theory-Based Flux Splitting Method for Ideal Magnetohydrodynamics

Kun Xu

Mathematics Department, The Hong Kong University of Science & Technology,
Clear Water Bay, Kowloon, Hong Kong
E-mail: makxu@uxmail.ust.hk

A gas-kinetic flux splitting method is developed for the ideal magnetohydrody-
namics (MHD) equations. The new scheme is based on the direct splitting of the
flux function of the MHD equations with the inclusion of "particle" collisions in the
transport process. Consequently, the artificial dissipation in the new scheme is greatly
reduced in comparison with the MHD flux vector splitting method. Numerical results
from the current scheme are favorable compared with those from the well-developed
Roe-type MHD solver. In the current paper, the general principle of splitting the
macroscopic flux function based on the gas-kinetic theory is presented. The flux
construction strategy may shed some light on the possible construction of accurate
and robust hybrid schemes for the compressible flow simulations.   © 1999 Academic Press

Key Words: magnetohydrodynamics; flux splitting; gas-kinetic scheme.

1. INTRODUCTION

The development of numerical methods for the magnetohydrodynamics (MHD) equa-
tions has attracted much attention in recent years. Godunov-type schemes are considered
particularly useful here. On the basis of Roe's method [24], Brio and Wu developed the first
flux difference splitting (FDS) scheme for MHD equations [3]. Aslan also followed the idea
of fluctuation approach to construct a second-order upwind MHD solver [1]. Zachary *et al.*
applied an operator splitting technique and devised a high-order Godunov-type method
[35]. During the same period, multidimensional extension of MHD solvers was done by
Ryu *et al.* [25] and Tanaka [28]. On the basis of the nonlinear Riemann solver, Dai and
Woodward extended the PPM method there [6]. Powell *et al.* constructed an eight-wave
family eigensystem for the approximate Riemann solver [20, 21]. Most recently, based on
the Lax–Friedrichs flux splitting technique, Jiang and Wu applied a high-order WENO inter-
polation scheme to the MHD equations [12]. In order to increase the robustness and simplify
the complicated Roe-type MHD solver, Linde developed an adequate Riemann solver based

on the HLL method for heliosphere applications [13]. A majority of the methods mentioned above applied characteristic decomposition for the MHD waves, where the entropy, slow, Alfven, and fast waves have to be considered in the evaluation of a single flux function. Because of the wave decomposition procedure, considerable work is required to evaluate and justify the MHD eigensystem, where the nonstrict hyperbolicity causes additional difficulty [18]. For the same reason, issues related to the direct extension of the flux vector splitting (FVS) scheme to MHD equations have not been fully addressed. The search for robust, accurate, and efficient MHD flow solvers is still one of the primary directions in MHD research.

For the Euler and Navier–Stokes equations, the development of gas-kinetic schemes has also attracted attention [32]. A particular strength of kinetic schemes lies precisely where Godunov-type FDS schemes often fail, such as with carbuncle phenomena, positivity, and entropy conditions [8, 14, 23, 33]. However, like any other FVS method, the kinetic flux vector splitting (KFVS) scheme is very diffusive and less accurate in comparison with the Roe-type Riemann solver, especially for shear and contact waves. The diffusivity of the FVS schemes, such as Steger–Warming, van Leer, and the KFVS [22, 27, 31] is mainly due to the particle or wave free transport mechanism, which automatically sets the CFL time step equal to particle collision time. Consequently, the artificial viscosity coefficient is always proportional to the time step. Even though numerically the high-order FVS methods can obtain crisp shock resolution by using a MUSCL-type reconstruction method, physically it is impossible to develop a second-order FVS scheme for the inviscid Euler equations without correcting the free transport mechanism. In order to reduce the diffusivity, particle collisions have to be modeled and implemented in the gas evolution stage, such as that in the BGK scheme [34].

The construction of a gas-kinetic FVS scheme for the MHD equations began with Croisille *et al.* [5], where a MHD KFVS solver was obtained by simply extending the KFVS flux function of the Euler equations. The above MHD KFVS scheme is very robust and reliable, but overdiffusive, especially in the contact discontinuity regions [13]. Recently, another interesting gas-kinetic MHD solver has been developed by Huba and Lyon [9]. Different from the earlier approach, with this solver Huba and Lyon constructed two equilibrium states and a transport equation to recover the MHD equations. An important aspect of this method is that it provides a framework in which to incorporate additional terms into the MHD equations, e.g., anisotropic ion stress tensor and anisotropic temperature distribution. However, the physical basis of the transport equation and the reliability of the equilibrium states need to be further investigated. Since Huba and Lyon's flux function retains the FVS nature, large numerical dissipation is expected.

In this paper, we construct a new kinetic flux splitting method for MHD equations. Based on the BGK-type formulation, the KFVS MHD solver of Croisille *et al.* is generalized by including particle collisions. As a result, the new scheme reduces numerical dissipation significantly and gives a more accurate representation of wave interactions. In Section 3, it will be seen that the new scheme compares well with the Roe-type MHD solver [3, 21]. The flux construction method presented in this paper splits the macroscopic flux function directly; therefore, it is very useful in the design of numerical methods for complicated hyperbolic systems.

2. GAS-KINETIC APPROACH TO MHD EQUATIONS

In the one-dimensional case, the MHD equation

$$q_t + F(q)_x = 0$$

has the form [3]

$$\rho_t + (\rho U)_x = 0,$$
$$(\rho U)_t + (\rho U^2 + p_* - B_x^2)_x = 0,$$
$$(\rho V)_t + (\rho U V - B_x B_y)_x = 0,$$
$$(\rho W)_t + (\rho U W - B_x B_z)_x = 0, \tag{2.1}$$
$$(B_y)_t + (B_y U - B_x V)_x = 0,$$
$$(B_z)_t + (B_z U - B_x W)_x = 0,$$
$$(\rho \epsilon)_t + ((\rho \epsilon + p_*)U - B_x(B_x U + B_y V + B_z W))_x = 0,$$

where p_* is the total pressure

$$p_* = p + \frac{1}{2}(B_x^2 + B_y^2 + B_z^2),$$

and p is the gas pressure. The total energy density includes kinetic, thermal, and magnetic energy densities,

$$\rho \epsilon = \frac{1}{2}\rho(U^2 + V^2 + W^2) + \rho e + \frac{1}{2}(B_x^2 + B_y^2 + B_z^2).$$

For an ideal gas in equilibrium, the thermal energy is related to pressure through the relation

$$\rho e = p/(\gamma - 1).$$

Due to different physical origins, it should be emphasized that in order to properly split the energy flux function, the splitting of internal energy flux $\rho e U$ and the splitting of work done by the pressure pU should be different, although they are only different by a constant $1/(\gamma - 1)$ for the ideal gas.

Theoretically, it is very difficult to construct an equilibrium state and a single kinetic transport equation to exactly recover the above ideal MHD equations. Basically, Faraday's law for the time evolution of magnetic field comes from the Maxwell equations and there is no corresponding "particle" picture in representing the field evolution. However, instead of constructing the equilibrium distribution for the flow and magnetic field, we can split the MHD flux function directly on the macroscopic level using gas-kinetic theory.

2.1. Gas-Kinetic Flux Splitting Method

In gas-kinetic theory, the flux is associated with the particle motion across a cell interface. For a 1D flow in the x-direction, the particle motion in this direction determines the flux function. Other quantities, such as the y-direction velocity, thermal energy, and magnetic field, can be considered as passive scalars which are transported with the x-direction particle velocity. Normally, particles are randomly distributed around the average velocity. From statistical mechanics, the moving particles in the x-direction can be most favorably described by the Maxwell–Boltzmann distribution function,

$$g = \rho \left(\frac{\lambda}{\pi}\right)^{1/2} e^{-\lambda(u-U)^2}, \tag{2.2}$$

where U is the average velocity and λ is the normalization factor of the distribution of random velocity. Note that λ is related to the temperature of the gas flow, i.e., $\lambda = m/2kT$, where m is the molecular mass, k is the Boltzmann constant, and T is the temperature.

The transport of any flow quantity is basically due to the movement of particles. With the above equilibrium state g, we can split the particles into two groups. One group is moving to the right with $u > 0$, and the other group is moving to the left with $u < 0$. Before splitting the fluxes, let us first define the moments of the particle distribution function,

$$\langle u^n \rangle = \int u^n \left(\frac{\lambda}{\pi} \right)^{1/2} e^{-\lambda(u-U)^2} \, du,$$

where the integration limit of the particle velocity u can be $(-\infty, +\infty)$, $(-\infty, 0)$, or $(0, +\infty)$. There is a recursive relation for the moments $\langle u^n \rangle$, which is

$$\langle u^{n+2} \rangle = U \langle u^{n+1} \rangle + \frac{n+1}{2\lambda} \langle u^n \rangle.$$

In order to simplify the presentation, we define the notations

$$\langle \cdots \rangle = \int_{-\infty}^{\infty} (\cdots) \left(\frac{\lambda}{\pi} \right)^{1/2} e^{-\lambda(u-U)^2} \, du,$$

$$\langle \cdots \rangle_+ = \int_0^{\infty} (\cdots) \left(\frac{\lambda}{\pi} \right)^{1/2} e^{-\lambda(u-U)^2} \, du,$$

and

$$\langle \cdots \rangle_- = \int_{-\infty}^0 (\cdots) \left(\frac{\lambda}{\pi} \right)^{1/2} e^{-\lambda(u-U)^2} \, du.$$

For example, we have

$$\langle u^0 \rangle_+ = \frac{1}{2} \mathrm{erfc}(-\sqrt{\lambda}U); \qquad \langle u^0 \rangle_- = \frac{1}{2} \mathrm{erfc}(\sqrt{\lambda}U),$$

where erfc is the complementary error function, and

$$\langle u^1 \rangle_+ = U \langle u^0 \rangle_+ + \frac{1}{2} \frac{e^{-\lambda U^2}}{\sqrt{\pi \lambda}}; \qquad \langle u^1 \rangle_- = U \langle u^0 \rangle_- - \frac{1}{2} \frac{e^{-\lambda U^2}}{\sqrt{\pi \lambda}}.$$

Obviously, if the integration limit is $(-\infty, \infty)$, the following relations hold:

$$\langle u^0 \rangle = 1, \qquad \langle u^1 \rangle = U.$$

Depending on the particle moving direction, the total density ρ can be split into

$$\rho^+ = \int_0^{\infty} g \, du$$
$$= \rho \langle u^0 \rangle_+$$

and

$$\rho^- = \int_{-\infty}^0 g \, du$$
$$= \rho \langle u^0 \rangle_-.$$

Any macroscopic quantity Z without containing explicitly the x-component velocity U, such as the density ρ, y-, and z-direction momentum ρV and ρW, and magnetic field $B_x B_y$, can be split similarly:

$$Z^+ = Z \langle u^0 \rangle_+$$

and

$$Z^- = Z \langle u^0 \rangle_-.$$

The above relations mean that the quantity Z is simply advected with the particle transport in the x-direction.

The x-direction momentum ρU can be split into

$$(\rho U)^+ = \int_0^\infty u g \, du$$
$$= \rho \langle u^1 \rangle_+$$

and

$$(\rho U)^- = \int_{-\infty}^0 u g \, du$$
$$= \rho \langle u^1 \rangle_-.$$

Similarly, any quantity containing the U term, such as $B_x U$, $B_y U$, ρU, $\rho V U$, and $\rho W U$, can be split as

$$(ZU)^+ = Z \langle u^1 \rangle_+$$

and

$$(ZU)^- = Z \langle u^1 \rangle_-.$$

For the magnetic field, the above splitting implies that the field is frozen into the particle motion and transported with the fluid. Note that ZU does not include pU, and the splitting of pU will be derived later.

The energy can be split into two terms $(\rho \epsilon)^+$ and $(\rho \epsilon)^-$, where

$$(\rho \epsilon)^+ = \int_0^\infty \frac{1}{2} u^2 g \, du$$
$$= \frac{1}{2} \langle u^2 \rangle_+$$
$$= \frac{1}{2} \rho U \langle u^1 \rangle_+ + \frac{\rho}{4\lambda} \langle u^0 \rangle_+$$
$$= \frac{1}{2} \rho U \langle u^1 \rangle_+ + \rho e \langle u^0 \rangle_+,$$

where ρe is the thermal energy of the specific distribution function g in Eq. (2.2) with the value of $\rho/4\lambda$. Similarly, we have

$$
\begin{aligned}
(\rho\epsilon)^- &= \int_{-\infty}^{0} \frac{1}{2} u^2 g \, du \\
&= \frac{1}{2} \langle u^2 \rangle_- \\
&= \frac{1}{2} \rho U \langle u^1 \rangle_- + \frac{\rho}{4\lambda} \langle u^0 \rangle_- \\
&= \frac{1}{2} \rho U \langle u^1 \rangle_- + \rho e \langle u^0 \rangle_-.
\end{aligned}
$$

The above equations imply that the kinetic energy $\frac{1}{2}\rho U^2$ can be split as

$$
\begin{aligned}
\frac{1}{2}\rho U^2 &= \left(\frac{1}{2}\rho U^2\right)^+ + \left(\frac{1}{2}\rho U^2\right)^- \\
&= \frac{1}{2}\rho U \langle u^1 \rangle_+ + \frac{1}{2}\rho U \langle u^1 \rangle_-,
\end{aligned}
$$

and the thermal energy can also be split as

$$
\begin{aligned}
\rho e &= (\rho e)^+ + (\rho e)^- \\
&= \rho e \langle u^0 \rangle_+ + \rho e \langle u^0 \rangle_-.
\end{aligned}
$$

In addition to the thermal energy, we can also use the above formulation to split the other quantities without an explicit macroscopic velocity dependence, such as magnetic energy in the MHD equations. For nonideal gases, the internal energy could be a complicated function of ρ and T. The above formulation can still be used to split it in terms of $\langle u^0 \rangle_+$ and $\langle u^0 \rangle_-$. For example, due to the relation between the pressure p and the thermal energy, the pressure can be split as

$$
p = p \langle u^0 \rangle_+ + p \langle u^0 \rangle_-.
$$

Now let us consider the energy transport. The energy transport in the positive x-direction is

$$
\begin{aligned}
\int_{0}^{\infty} \frac{1}{2} u^3 g \, du &= \frac{1}{2} \langle u^3 \rangle_+ \\
&= \left(\frac{1}{2}\rho U^2 + \rho e\right) \langle u^1 \rangle_+ + \frac{1}{2} U p \langle u^0 \rangle_+ + \frac{1}{2} p \langle u^1 \rangle_+ \\
&= \rho\epsilon \langle u^1 \rangle_+ + \frac{1}{2} U p \langle u^0 \rangle_+ + \frac{1}{2} p \langle u^1 \rangle_+,
\end{aligned}
$$

where $\rho\epsilon = \frac{1}{2}\rho U^2 + \rho e$ is the total energy density for the specific distribution g. Similarly,

the corresponding flux in the negative x-direction is

$$\int_{-\infty}^{0} \frac{1}{2} u^3 g \, du = \frac{1}{2} \langle u^3 \rangle_-$$

$$= \left(\frac{1}{2} \rho U^2 + \rho e \right) \langle u^1 \rangle_- + \frac{1}{2} U p \langle u^0 \rangle_- + \frac{1}{2} p \langle u^1 \rangle_-$$

$$= \rho \epsilon \langle u^1 \rangle_- + \frac{1}{2} U p \langle u^0 \rangle_- + \frac{1}{2} p \langle u^1 \rangle_-.$$

Since the total energy flux in the x-direction is

$$\int_{-\infty}^{\infty} \frac{1}{2} u^3 g \, du = \left(\frac{1}{2} \rho U^2 + \rho e \right) U + p U$$

$$= \rho \epsilon U + p U,$$

from the above three equations, we conclude that the total energy transport $\rho \epsilon U$ can be split as

$$\rho \epsilon U = (\rho \epsilon U)^+ + (\rho \epsilon U)^-$$

$$= \rho \epsilon \langle u^1 \rangle_+ + \rho \epsilon \langle u^1 \rangle_-.$$

Hence $\rho \epsilon U$ is composed of a kinetic energy transport splitting

$$\frac{1}{2} \rho U^3 = \left(\frac{1}{2} \rho U^3 \right)^+ + \left(\frac{1}{2} \rho U^3 \right)^-$$

$$= \frac{1}{2} \rho U^2 \langle u^1 \rangle_+ + \frac{1}{2} \rho U^2 \langle u^1 \rangle_-$$

and a thermal energy transport splitting

$$\rho e U = \rho e \langle u^1 \rangle_+ + \rho e \langle u^1 \rangle_-.$$

At the same time, the splitting of the work done by the pressure term pU becomes

$$pU = (pU)^+ + (pU)^-$$

$$= \frac{1}{2} (U p \langle u^0 \rangle_+ + p \langle u^1 \rangle_+) + \frac{1}{2} (U p \langle u^0 \rangle_- + p \langle u^1 \rangle_-).$$

Note that the above splitting formula can be generalized to a hyperbolic system with a complicated total energy density.

As a special application of the above splitting principle, let us split the 1D Euler fluxes. The flux function for the 1D Euler equations can be separated into

$$\begin{pmatrix} \rho U \\ \rho U^2 + p \\ \rho \epsilon U + p U \end{pmatrix} = F_f^+ + F_f^-,$$

where f means free transport. The positive flux F_f^+ is

$$F_f^+ = \langle u^1 \rangle_+ \begin{pmatrix} \rho \\ \rho U \\ \rho \epsilon \end{pmatrix} + \begin{pmatrix} 0 \\ p \langle u^0 \rangle_+ \\ \frac{1}{2} p \langle u^1 \rangle_+ + \frac{1}{2} p U \langle u^0 \rangle_+ \end{pmatrix},$$

and the negative part F_f^- is

$$F_f^- = \langle u^1 \rangle_- \begin{pmatrix} \rho \\ \rho U \\ \rho \epsilon \end{pmatrix} + \begin{pmatrix} 0 \\ p \langle u^0 \rangle_- \\ \frac{1}{2} p \langle u^1 \rangle_- + \frac{1}{2} p U \langle u^0 \rangle_- \end{pmatrix}.$$

With the above formulas, the flux across a cell interface $j + \frac{1}{2}$ for the Euler equations can be written as

$$F_{j+1/2}^f = F_{j,f}^+ + F_{j+1,f}^-.$$

This is exactly the KFVS scheme for the Euler equations [4, 17, 22], and the positivity and entropy condition for the above scheme have been analyzed by many authors; see [16, 19, 29] and references therein.

As analyzed in [32], all FVS schemes based on positive (negative) particle velocities suffer from the same weakness. The particle free transport across cell interfaces unavoidably introduces large numerical dissipation, and the viscosity and heat conduction coefficients are proportional to the CFL time step. In order to reduce the overdiffusivity in the FVS schemes, particle collisions have to be added in the transport process. On the other hand, the particle collisions can be used to simulate the physical diffusion in regions where the dissipative structure can be well resolved.

As a simple particle collisional model, we can imagine that the particles from the left- and right-hand sides of a cell interface collapse totally to form an equilibrium state. In order to define the equilibrium state at the cell interface, we need first to determine the corresponding macroscopic quantities $\bar{q}_{j+1/2}$ there. They are the total mass, momentum, and energy densities of the collapsed left and right moving beams. For example, for the Euler equations, we have

$$\bar{q}_{j+1/2} = \begin{pmatrix} \bar{\rho} \\ \bar{\rho} \bar{U} \\ \bar{\rho} \bar{\epsilon} \end{pmatrix}_{j+1/2}$$

$$= \begin{pmatrix} \rho \\ \rho U \\ \rho \epsilon \end{pmatrix}_j^+ + \begin{pmatrix} \rho \\ \rho U \\ \rho \epsilon \end{pmatrix}_{j+1}^-$$

$$= \begin{pmatrix} \rho \langle u^0 \rangle_+ \\ \rho \langle u^1 \rangle_+ \\ \left(\rho \epsilon - \frac{1}{2} \rho U^2 \right) \langle u^0 \rangle_+ + \frac{1}{2} \rho U \langle u^1 \rangle_+ \end{pmatrix}_j$$

$$+ \begin{pmatrix} \rho \langle u^0 \rangle_- \\ \rho \langle u^1 \rangle_- \\ \left(\rho \epsilon - \frac{1}{2} \rho U^2 \right) \langle u^0 \rangle_- + \frac{1}{2} \rho U \langle u^1 \rangle_- \end{pmatrix}_{j+1},$$

where $(\rho \epsilon - \frac{1}{2} \rho U^2)$ is the thermal energy density ρe. Then, from the "averaged" macroscopic flow quantities in the above equation, we can construct the corresponding equilibrium

flux function

$$F^e_{j+1/2} = \begin{pmatrix} \bar{\rho}\bar{U} \\ \bar{\rho}\bar{U}^2 + \bar{p} \\ (\bar{\rho}\bar{\epsilon} + \bar{p})\bar{U} \end{pmatrix}_{j+1/2}.$$

The final flux with the inclusion of both free transport (nonequilibrium) and collision (equilibrium) terms is

$$F_{j+1/2} = \eta F^f_{j+1/2} + (1 - \eta)F^e_{j+1/2},$$

where η is a justifiable parameter. The scheme with a fixed $\eta \in [0, 1]$ is called the partial thermalized transport method, which is exactly the first-order BGK scheme [32]. With the inclusion of the equilibrium flux function, the dissipation in the KFVS scheme is reduced substantially. In contrast to Roe's approximate Riemann solver for the Euler equations [24], the above BGK method strives to require even less information to form a flux function. As a result, the above scheme is very efficient. The construction of the $\bar{q}_{j+1/2}$ term at the cell interface has similar physical spirit as the evaluation of the Mach number and the flow velocity at the cell interfaces in the AUSM- and CUSP-type schemes [11, 15, 26]. In the next section, we extend the above method to the MHD equations.

2.2. Flux Splitting Method for MHD Equations

For MHD equations, we can use the same technique in the previous section to split the flux directly. The splitting of fluxes is closely related to the definition of $\langle u^0 \rangle$ and $\langle u^1 \rangle$ terms, which are functions of the x-direction velocity U and the "temperature" λ. For MHD equations, both gas and magnetic fields contribute to the total pressure p_*. With the definition of normal pressure from the distribution function g,

$$p = \int_{-\infty}^{\infty} (u - U)^2 g \, du = \frac{\rho}{2\lambda},$$

the total pressure (gas + magnetic) in the MHD equations uniquely determines the value of λ,

$$\lambda = \frac{\rho}{2p_*} = \frac{\rho}{2p + \left(B_x^2 + B_y^2 + B_z^2\right)},$$

where p is the gas pressure. The velocity U in g can be the same as the macroscopic fluid velocity in the x-direction.

After determining λ and U, we can calculate the moments of $\langle u^0 \rangle$ and $\langle u^1 \rangle$, and we are ready to split the MHD flux function,

$$F = \begin{pmatrix} \rho U \\ \rho U^2 + p_0 \\ \rho U V - B_x B_y \\ \rho U W - B_x B_z \\ B_y U - B_x V \\ B_z U - B_x W \\ \rho \epsilon U + p_0 U - B_x (B_y V + B_z W) \end{pmatrix} = F^+_f + F^-_f,$$

where $p_0 = p_* - B_x^2$. The positive flux F_f^+ is

$$
F_f^+ = \langle u^1 \rangle_+ \begin{pmatrix} \rho \\ \rho U \\ \rho V \\ \rho W \\ B_y \\ B_z \\ \rho \epsilon \end{pmatrix} + \begin{pmatrix} 0 \\ p_0 \langle u^0 \rangle_+ \\ -B_x B_y \langle u^0 \rangle_+ \\ -B_x B_z \langle u^0 \rangle_+ \\ -B_x V \langle u^0 \rangle_+ \\ -B_x W \langle u^0 \rangle_+ \\ \frac{1}{2} \left(p_0 U \langle u^0 \rangle_+ + p_0 \langle u^1 \rangle_+ \right) - B_x (B_y V + B_z W) \langle u^0 \rangle_+ \end{pmatrix}.
$$

Similarly, the negative flux is

$$
F_f^- = \langle u^1 \rangle_- \begin{pmatrix} \rho \\ \rho U \\ \rho V \\ \rho W \\ B_y \\ B_z \\ \rho \epsilon \end{pmatrix} + \begin{pmatrix} 0 \\ p_0 \langle u^0 \rangle_- \\ -B_x B_y \langle u^0 \rangle_- \\ -B_x B_z \langle u^0 \rangle_- \\ -B_x V \langle u^0 \rangle_- \\ -B_x W \langle u^0 \rangle_- \\ \frac{1}{2} \left(p_0 U \langle u^0 \rangle_- + p_0 \langle u^1 \rangle_- \right) - B_x (B_y V + B_z W) \langle u^0 \rangle_- \end{pmatrix}.
$$

When we combine the above splitting fluxes, the free transport flux for the MHD equations at a cell interface becomes

$$
F_{j+1/2}^f = F_{j,f}^+ + F_{j+1,f}^-.
$$

This formulation is exactly the one given by Croisille *et al.* [5]. Numerically, the above flux function is very reliable and robust [13], and the scheme performs well for problems where the Roe scheme fails, such as in the cases of the odd–even decoupling and carbuncle phenomena [8, 13, 23]. However, the accuracy of the above scheme is noticeably worse, especially around contact and tangential discontinuities in MHD applications.

Now let us construct the corresponding equilibrium flux for the MHD equations. The corresponding macroscopic variables of an equilibrium state at a cell interface are

$$
\bar{q}_{j+1/2} = \begin{pmatrix} \bar{\rho} \\ \bar{\rho} \bar{U} \\ \bar{\rho} \bar{V} \\ \bar{\rho} \bar{W} \\ \bar{B}_y \\ \bar{B}_z \\ \bar{\rho} \bar{\epsilon} \end{pmatrix}_{j+1/2} = q_j^+ + q_{j+1}^-, \tag{2.3}
$$

where

$$
q_j^+ = \begin{pmatrix}
\rho \langle u^0 \rangle_+ \\
\rho \langle u^1 \rangle_+ \\
\rho V \langle u^0 \rangle_+ \\
\rho W \langle u^0 \rangle_+ \\
B_y \langle u^0 \rangle_+ \\
B_z \langle u^0 \rangle_+ \\
\left(\rho \epsilon - \frac{1}{2} \rho U^2 \right) \langle u^0 \rangle_+ + \frac{1}{2} \rho U \langle u^1 \rangle_+
\end{pmatrix}_j ,
$$

and

$$
\bar{q}_{j+1} = \begin{pmatrix}
\rho \langle u^0 \rangle_- \\
\rho \langle u^1 \rangle_- \\
\rho V \langle u^0 \rangle_- \\
\rho W \langle u^0 \rangle_- \\
B_y \langle u^0 \rangle_- \\
B_z \langle u^0 \rangle_- \\
\left(\rho \epsilon - \frac{1}{2} \rho U^2 \right) \langle u^0 \rangle_- + \frac{1}{2} \rho U \langle u^1 \rangle_-
\end{pmatrix}_{j+1} .
$$

With the above averaged macroscopic variables $\bar{q}_{j+1/2}$, the equilibrium flux can be constructed as

$$
F_{j+1/2}^e = F(\bar{q}_{j+1/2}) = \begin{pmatrix}
\bar{\rho} \bar{U} \\
\bar{\rho} \bar{U}^2 + \bar{p}_* - \bar{B}_x^2 \\
\bar{\rho} \bar{U} \bar{V} - \bar{B}_x \bar{B}_y \\
\bar{\rho} \bar{U} \bar{W} - \bar{B}_x \bar{B}_z \\
\bar{B}_y \bar{U} - \bar{B}_x \bar{V} \\
\bar{B}_z \bar{U} - \bar{B}_x \bar{W} \\
(\bar{\rho} \bar{\epsilon} + \bar{p}_*) \bar{U} - \bar{B}_x (\bar{B}_x \bar{U} + \bar{B}_y \bar{V} + \bar{B}_z \bar{W})
\end{pmatrix}_{j+1/2} ,
$$

where $\bar{B}_x = B_x$ is a constant in the 1D case and

$$
\bar{p}_* = (\gamma - 1) \left(\bar{\rho} \bar{\epsilon} - \frac{1}{2} \bar{\rho} (\bar{U}^2 + \bar{V}^2 + \bar{W}^2) - \frac{1}{2} \left(\bar{B}_x^2 + \bar{B}_y^2 + \bar{B}_z^2 \right) \right) + \frac{1}{2} \left(\bar{B}_x^2 + \bar{B}_y^2 + \bar{B}_z^2 \right).
$$

The final flux function across a cell interface is a combination of nonequilibrium and equilibrium flux functions

$$
F_{j+1/2} = \eta F_{j+1/2}^f + (1 - \eta) F_{j+1/2}^e, \tag{2.4}
$$

where η is an adaptive parameter. The program from the left and right states q_j and q_{j+1} to the final flux function $F_{j+1/2}$ is given in the Appendix. By removing the contribution from the magnetic field, the above MHD flux function reduces exactly to the BGK flux constructed for the Euler equations in the previous section.

In the current study, we are more interested in the construction of a flux function for the MHD equations. For the first-order scheme, η can be fixed, at, say, 0.7 or 0.5, in the numerical calculations. Theoretically, the parameter η should depend on the real flow situations: in equilibrium and smooth flow regions, the use of $\eta \sim 0$ is physically reasonable, and in regions with discontinuities, η should be close to 1 in order to have enough numerical dissipation to recover the smooth shock transition. A possible choice for the construction of η is to design a pressure-based stencil, such as the pressure switch function in the Jameson–Schmidt–Turkel scheme [10]. In a high-order BGK scheme for the Euler and Navier–Stokes equations [32], the time-dependent flux function can be obtained by following the BGK solution, and the relation between the collision time τ and viscosity coefficient is well established. On the contrary, for the MHD equations we only split the macroscopic flux function without knowing the explicit microscopic transport equation for the fluid and magnetic field. However, we can still follow the MUSCL-type approach to extend the current scheme to high order [30]. For example, we can get the left and right states at a cell interface through the nonlinear reconstruction of the initial data, and then evaluate the flux according to the formulation given by Eq. (2.4). A high-order Runge–Kutta time stepping scheme is also recommended.

3. A NUMERICAL EXPERIMENT

For any upwinding scheme, the construction of the flux function, or the first-order scheme, is very important in the understanding of the scheme. For high-order extensions, many factors, such as the nonlinear limiter, the reconstruction of conservative or primitive variables, and time stepping methods, can affect the performance of the scheme. In the following, we apply the current method to the Brio–Wu 1D MHD test case [3], where the results with fixed $\eta = 0.5$ will be presented.

The initial condition of the Brio–Wu case is

$$\rho_l = 1.0, \qquad U_l = 0, \qquad p_l = 1, \qquad B_{x,l} = 0.75, \qquad B_{y,l} = 1$$

on the left and

$$\rho_r = 0.125, \qquad U_l = 0, \qquad p_r = 0.1, \qquad B_{x,r} = 0.75, \qquad B_{y,r} = -1$$

on the right. The gas constant γ is equal to 2. Note that the gas-kinetic flux splitting formula presented in the last section can be applied for any reasonable γ.

In order to evaluate the performance of the current method, we compare its numerical results with those from the Roe-type MHD Riemann solver [3, 21]. The Roe-type MHD solver is considered the most accurate MHD solver existing so far [13], although the robustness of the scheme is questionable in some special applications.

There are 400 grid points used from $[-1, 1]$ in the x-direction. The time step is based on $\Delta t / \Delta x = 0.2$, which is equivalent to CFL number 0.8 in this case. The results of the first-order scheme at 200 time steps are displayed in Figs. 1–5. The results from the first-order Roe scheme [3, 21], with identical initial condition and time step, are also plotted in these figures. In most regions, the kinetic and Roe-type MHD solvers give almost identical results, except the nonconservative quantities at the fast right moving rarefaction wave.

Due to the nonconvexity of the MHD equations, compound waves, which directly connect shock and rarefaction waves, may be present. In Table 1, we list the data at the peak point of

TABLE 1
Flow Variables at the Peak Point of Compound Wave

Scheme	ρ	U-velocity	V-velocity	B_y	Gas pressure p
Theory [3]	0.7935	0.4983	−1.290	−0.3073	0.6687
Kinetic	0.8179	0.4679	−1.083	−0.1239	0.7300
Roe	0.8257	0.4623	−0.928	0.0163	0.7400
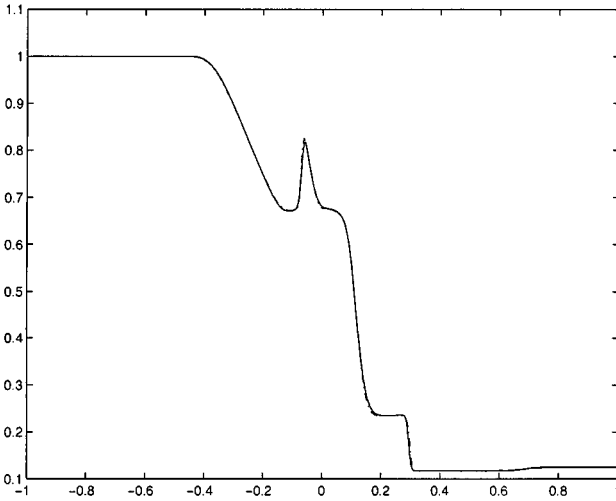
FIG. 1. Density distributions with 400 grid points. Solid line: first-order BGK-type scheme. Dash/dot line: first-order Roe-MHD solver.
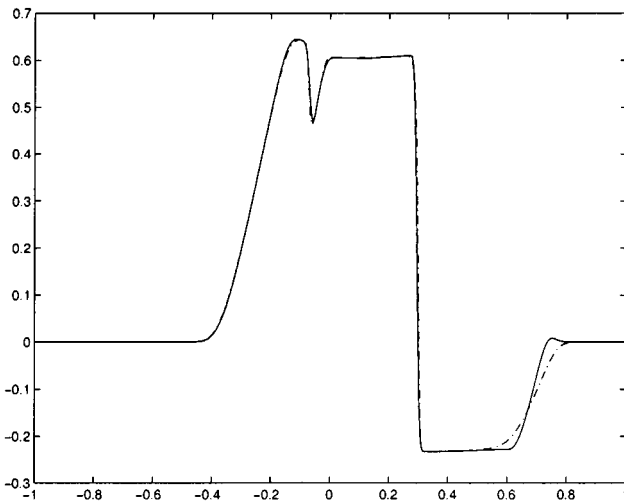
FIG. 2. x-component velocity distributions with 400 grid points. Solid line: first-order BGK-type scheme. Dash/dot line: first-order Roe-MHD solver.
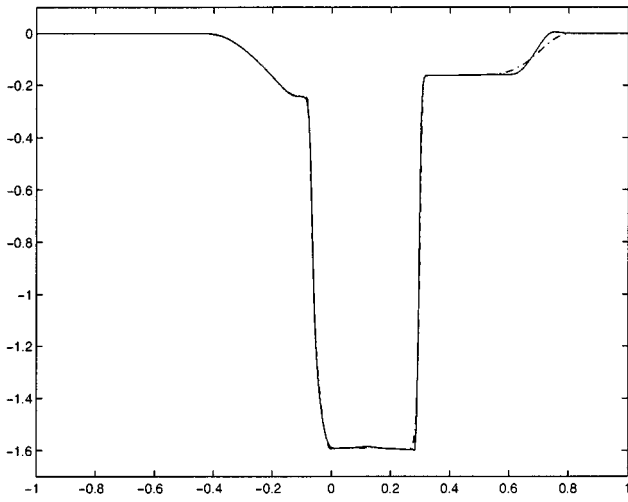
FIG. 3. *y*-component velocity distributions with 400 grid points. Solid line: first-order BGK-type scheme. Dash/dot line: first-order Roe-MHD solver.
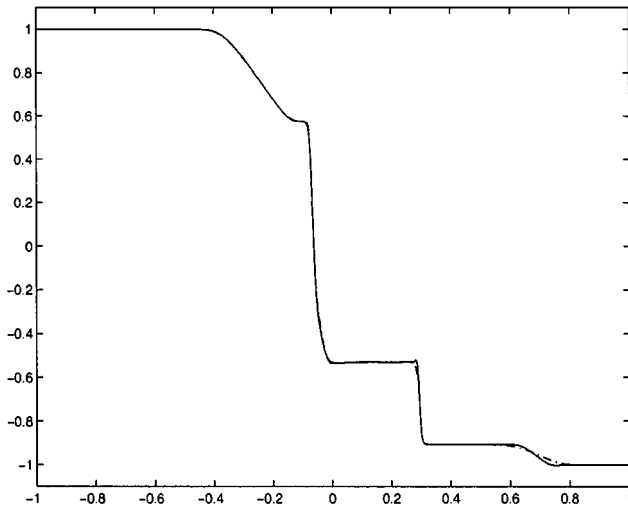

FIG. 4. B_y distributions with 400 grid points. Solid line: first-order BGK-type scheme. Dash/dot line: first-order Roe-MHD solver.
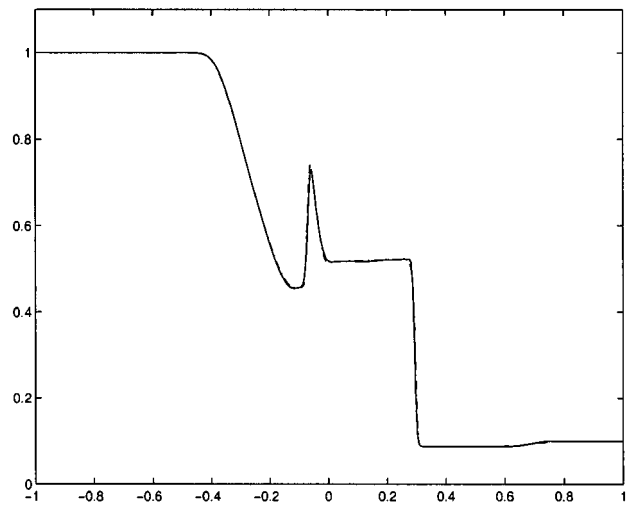

FIG. 5. Gas pressure *p* distributions with 400 grid points. Solid line: first-order BGK-type scheme. Dash/dot line: first-order Roe-MHD solver.
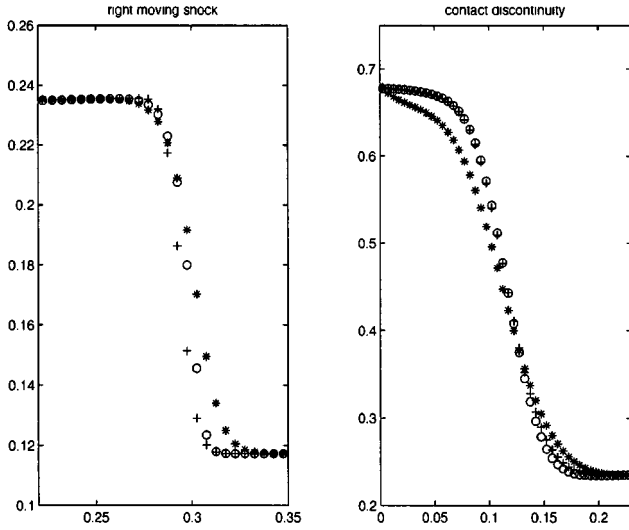
FIG. 6. Density profiles around right moving shock and middle contact discontinuity using three first-order schemes. (+) Current kinetic method with $\eta = 0.5$. (◯) Roe-type MHD solver. (∗) KFVS MHD solver of Croisille *et al.* (corresponding to $\eta = 1.0$ in the current scheme).

the compound wave in the Brio–Wu test case. Both results are compared with the theoretical prediction in [3]. Figure 6 gives a close look at the density distributions around the right moving shock and the middle contact discontinuity wave. Three schemes used here are the current one with $\eta = 0.5$, the KFVS MHD solver of Croisille *et al.*, and the Roe-type MHD solver. The diffusivity of the KFVS MHD solver can clearly be observed.

In order to reduce the numerical dissipation, a MUSCL-type technique can be used to extend the current scheme to second-order accuracy [30]. For the same initial condition, we now use the van Leer limiter to construct two constant states around a cell interface,

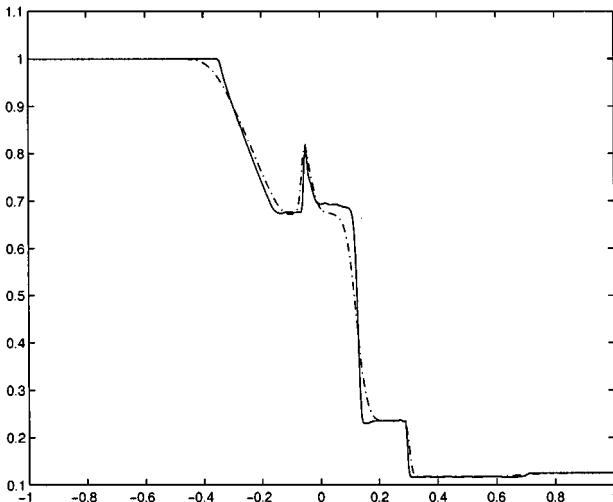$$q^l_{j+1/2} \qquad \text{and} \qquad q^r_{j+1/2},$$

FIG. 7. Density distributions with 400 grid points. Solid line: second-order BGK-type scheme (Eq. (3.5)). Dash/dot line: first-order BGK-type scheme (Eq. (2.4)).

and use the same procedure presented in this paper to evaluate the numerical fluxes. The flow variables inside each cell is simply updated by the one-step Euler method,

$$q_j^{n+1} = q_j^n + \frac{\Delta t}{\Delta x} \left(F_{j-1/2} \left(q_{j-1/2}^l, q_{j-1/2}^r \right) - F_{j+1/2} \left(q_{j+1/2}^l, q_{j+1/2}^r \right) \right). \tag{3.5}$$

The density distribution is shown in Fig. 7, from which we can clearly observe that the second-order interpolation resolves the flow sctructures better, especially for the contact discontinuity wave. At the same time, the smoothness of the solution is reduced.

4. DISCUSSION AND CONCLUSION

In this paper, we have constructed the kinetic flux splitting formula for the MHD equations based on the gas-kinetic theory. We feel that there are many applications of the splitting techniques presented in this paper. Also, the kinetic flux splitting formulation has similarities with the AUSM- and CUSP-type schemes [11, 15], where the advection and pressure terms are split differently. Numerical results validate the accuracy of the current approach.

In terms of the current gas-kinetic MHD solver, we have the following remarks:

(1) To get a truly multidimensional MHD solver is a formidable work. A direct way to extend the current method to the multidimensional case is to use the dimensional splitting technique, where the flow equations in the x-, y-, and z-directions are solved subsequently. If there is a jump of magnetic field in the normal direction, such as B_x in the x-direction across a cell interface, the weakly nonconservative form [21]

$$\frac{\partial B_x}{\partial t} + U \frac{\partial B_x}{\partial x} = 0$$

can be split by changing U in the above equation to $\bar{U}$ of Eq. (2.3). Also, in order to satisfy $\nabla \cdot \mathbf{B} = 0$ condition, the projection method can be used to clean up the nonzero divergence of the magnetic field [2].

(2) The current scheme is very efficient in comparison with the Roe-type Riemann MHD solver. For example, for 1D calculations, the flux evaluation takes about one-third the amount of CPU time as the Roe-type scheme. For 3D calculations, the saving of computational time is enormous. Since we do not use characteristic information of the MHD system, the numerical problems related to nonconvexity, nonstrict hyperbolicity, and linearization are avoided. Also, the Boltzmann-type scheme is very robust, especially for high-speed, low-density regions [13]. The main reason for this is that the splitting is based on $\langle u^n \rangle_+$ and $\langle u^n \rangle_-$, which accounts for all particle velocities, instead of switching the flux function according to the Mach number $M > 1$ or $M < 1$ in many other splitting schemes.

(3) The extension of the current method to the system with a general equation of state $p = p(\rho, e)$ is straightforward. The important point is to distinguish the differences between the splitting of internal energy flux $\rho e U$ and the work done by the pressure pU. No singularity and ambiguity in characteristic decomposition of the MHD equations will be encountered in the gas-kinetic splitting formulation.

There are still many open questions related to the current gas-kinetic approach. First, underlying the macroscopic flux splitting, we do not know the exact microscopic equilibrium state for the whole flow system including the gas and magnetic field. Second, different from

the BGK scheme for the Euler and Navier–Stokes equations [32], there is no direct way to extend the current method to solve dissipative (including resistivity and dispersive effects) MHD equations due to the lack of microscopic transport equations, although the dissipative terms can be regarded as additional source terms to the current ideal MHD equations. Third, in plasma calculations, the particle method is usually used [7]. How to make the smooth transition from the microscopic particle method to the macroscopic MHD Riemann solver through the gas-kinetic scheme is an important and interesting research topics. Even with many unknowns, the potential advantage of the kinetic approach over the Riemann solver in the construction of the numerical flux function becomes clear when solving increasingly more complicated hyperbolic systems.

APPENDIX: EVALUATION OF KINETIC MHD FLUX FUNCTION

```
c  gas constant GAM $\gamma$ and PI=3.14 $\pi$ given
c  left state  = (ADE1,AXM1,AYM1,AZM1,AEN1,ABX1,ABY1,ABZ1)
c which is $(\rho)_j, (\rho U)_j, (\rho  V)_j, (\rho W)_j,
c          (\rho \epsilon)_j, (B_x)_j, (B_y)_j, (B_z)_j $,
c  right state = (ADE2,AXM2,AYM2,AZM2,AEN2,ABX2,ABY2,ABZ2)
c which is $(\rho)_{j+1}, (\rho U)_{j+1}, (\rho  V)_{j+1}, (\rho W)_{j+1},
c          (\rho \epsilon)_{j+1}, (B_x)_{j+1}, (B_y)_{j+1}, (B_z)_{j+1} $
c  left and right pressures
        APP1=(GAM-1)*(AEN1-0.5*(AXM1**2+AYM1**2+AZM1**2)/ADE1)
     *       +0.5*(2.0-GAM)*(ABX1**2+ABY1**2+ABZ1**2)          | $p_j$
        APP2=(GAM-1)*(AEN2-0.5*(AXM2**2+AYM2**2+AZM2**2)/ADE2)
     *       +0.5*(2.0-GAM)*(ABX2**2+ABY2**2+ABZ2**2)          | $p_{j+1}$
c left and right $\lambda$, and macroscopic velocities ($U,V,W$)
        AE1=0.5*ADE1/APP1                             | $\lambda_j$
        AU1=AXM1/ADE1                                 | $U_j$
        AV1=AYM1/ADE1                                 | $V_j$
        AW1=AZM1/ADE1                                 | $W_j$
        AE2=0.5*ADE2/APP2                             | $\lambda_{j+1}$
        AU2=AXM2/ADE2                                 | $U_{j+1}$
        AV2=AYM2/ADE2                                 | $V_{j+1}$
        AW2=AZM2/ADE2                                 | $W_{j+1}$
c particle  velocity moments.
        TEU0=0.5*DERFC(-AU1*SQRT(AE1))               | $<u^0>_+ $
        TEU1=AU1*TEU0+0.50*EXP(-AE1*AU1*AU1)/SQRT(AE1*PI)   | $<u^1>_+ $
        TGU0=0.5*(DERFC(AU2*SQRT(AE2)))              | $<u^0>_- $
        TGU1=AU2*TGU0-0.50*EXP(-AE2*AU2*AU2)/SQRT(AE2*PI)   | $<u^1>_- $
c equilibrium state at the cell interface
        ADE=ADE1*TEU0+ADE2*TGU0                       | $\bar \rho$
        AU=(ADE1*TEU1+ADE2*TGU1)/ADE                  | $\bar U$
        AV=(ADE1*AV1*TEU0+ADE2*AV2*TGU0)/ADE          | $\bar V$
        AW=(ADE1*AW1*TEU0+ADE2*AW2*TGU0)/ADE          | $\bar W$
        ABY=ABY1*TEU0+ABY2*TGU0                        | $\bar B_y$
        ABZ=ABZ1*TEU0+ABZ2*TGU0                        | $\bar B_z$
        AE=(AEN1-0.5*ADE1*AU1**2)*TEU0+(AEN2-0.5*ADE2*AU2**2)*TGU0
     *       +0.5*ADE1*AU1*TEU1+0.5*ADE2*AU2*TGU1     | $\bar \lambda$
        TP=(GAM-1)*(AE-0.5*ADE*(AU**2+AV**2+AW**2))
     *       +0.5*(2.0-GAM)*(ABX1**2+ABY1**2+ABZ1**2) | $\bar p$
c gas-kinetic flux function, ETA $\eta$ is a justifiable parameter.
        FM=ETA*(TEU1*ADE1+TGU1*ADE2)+(1-ETA)*ADE*AU   | $F_{\rho}$
        FU=ETA*(TEU1*AXM1+TGU1*AXM2+(APP1-ABX1**2)*TEU0+(APP2-ABX2**2)*TGU0)
     *       +(1-ETA)*(ADE*AU**2+TP-ABX1**2)          | $F_{\rho U}$
        FV=ETA*(TEU1*AYM1+TGU1*AYM2-ABX1*ABY1*TEU0-ABX2*ABY2*TGU0)
     *       +(1-ETA)*(ADE*AU*AV-ABX1*ABY)            | $F_{\rho V}$
        FW=ETA*(TEU1*AZM1+TGU1*AZM2-ABX1*ABZ1*TEU0-ABX2*ABZ2*TGU0)
     *       +(1-ETA)*(ADE*AU*AW-ABX1*ABZ)            | $F_{\rho W}$
        FBY=ETA*(TEU1*ABY1+TGU1*ABY2-ABX1*AV1*TEU0-ABX2*AV2*TGU0)
     *       +(1-ETA)*(ABY*AU-ABX1*AV)                | $F_{B_y}$
        FBZ=ETA*(TEU1*ABZ1+TGU1*ABZ2-ABX1*AW1*TEU0-ABX2*AW2*TGU0)
     *       +(1-ETA)*(ABZ*AU-ABX1*AW)                | $F_{B_z}$
        FE=ETA*(TEU1*AEN1+TGU1*AEN2                   | $F_{\rho \epsilon}$
     *       +0.5*(APP1-ABX1**2)*TEU1+0.5*AU1*(APP1-ABX1**2)*TEU0
     *       -ABX1*(ABY1*AV1+ABZ1*AW1)*TEU0
     *       +0.5*(APP2-ABX2**2)*TGU1+0.5*AU2*(APP2-ABX2**2)*TGU0
     *       -ABX2*(ABY2*AV2+ABZ2*AW2)*TGU0)
     *       +(1-ETA)*((AE+TP)*AU-ABX1*(ABX1*AU+ABY*AV+ABZ*AW))
```

ACKNOWLEDGMENTS

REFERENCES

1. N. Aslan, Numerical solutions of one-dimensional MHD equations by a fluctuation approach, *Int. J. Numer. Meth. Fluids* **22**, 569 (1996).

2. J. U. Brackbill and D. C. Barnes, The effect of nonzero div **B** on the numerical solution of the magnetohydrodynamic equations, *J. Comput. Phys.* **35**, 426 (1980).

3. M. Brio and C. C. Wu, An upwind differencing schemes for the equations of ideal magnetohydrodynamics, *J. Comput. Phys.* **75**, 400 (1988).

4. S. Y. Chou and D. Baganoff, Kinetic flux-vector splitting for the Navier–Stokes equations, *J. Comput. Phys.* **130**, 217 (1997).

5. J.-P. Croisille, R. Khanfir, and G. Chanteur, Numerical simulation of the MHD equations by a kinetic-type method, *J. Sci. Comput.* **10**, 81 (1995).

6. W. Dai and P. Woodward, A high-order Godunov-type scheme for shock interactions in ideal magnetohydrodynamics, *SIAM J. Sci. Comput.* **18**, 957 (1997).

7. J. M. Dawson and A. T. Lin, Particle Simulation, in *Handbook of Plasma Physics* edited by A. A. Galeev and R. N. Sudan (Elsevier, Amsterdam, 1989), p. 461.

8. J. Gressier and J. M. Moschetta, *On the Pathological Behavior of Upwind Schemes*, AIAA 98-0110 (1998).

9. J. D. Huba and J. G. Lyon, *A New 3D MHD Algorithm: The Distribution Function Method*, submitted for publication.

10. A. Jameson, W. Schmidt, and E. Turkel, *Numerical Solutions of the Euler Equations by Finite Volume Methods Using Runge–Kutta Time-Stepping Schemes*, AIAA81-1259 (1981).

11. A. Jameson, Positive schemes and shock modeling for compressible flows, *Int. J. Numer. Meth. Fluids* **20**, 743 (1995).

12. G. S. Jiang and C. C. Wu, A high order WENO finite difference scheme for the equations of the ideal magnetohydrodynamics, *J. Comput. Phys.* **150**, 561 (1999).

13. T. J. Linde, *A Three-dimensional Adaptive Multifluid MHD Model of the Heliosphere*, Ph.D. Thesis (University of Michigan, 1998).

14. M. S. Liou, *Probing Numerical Fluxes, Positivity, and Entropy-Satisfying Property*, AIAA 97-2035 (1997).

15. M. S. Liou and C. J. Steffen, A new flux splitting scheme, *J. Comput. Phys.* **107**, 23 (1993).

16. S. H. Lui and K. Xu, *Entropy Analysis of Kinetic Flux Vector Splitting Schemes for the Compressible Euler Equations*, ICASE Report 99-5 (1999).

17. J. C. Mandal and S. M. Deshpande, Kinetic flux vector splitting for Euler equations, *Comput. Fluids* **23**, 447 (1994).

18. R. S. Myong and P. L. Roe, On Godunov-type schemes for magnetohydrodynamics. 1. A Model System, *J. Comput. Phys.* **147**, 545 (1998).

19. B. Perthame, Second-order Boltzmann schemes for compressible Euler equation in one and two space dimensions, *SIAM J. Numer. Anal.* **29** (1992).

20. K. G. Powell, *An Approximate Riemann Solver for Magnetohydrodynamics*, ICASE Report 94-24 (1994).

21. K. G. Powell, P. L. Roe, T. J. Linde, T. I. Gombosi, and D. L. DeZeeuw, A solution-adaptive upwind scheme for ideal magnetohydrodynamics, *J. Comput. Phys.*, in press.

22. D. I. Pullin, Direct simulation methods for compressible inviscid ideal gas flow, *J. Comput. Phys.* **34**, 231 (1980).

23. J. Quirk, A contribution to the great Riemann solver debate, *Int. J. Numer. Meth. Fluids* **18**, 555 (1994).

24. P. L. Roe, Approximate Riemann solvers, parameter vectors, and difference schemes, *J. Comput. Phys.* **43**, 357 (1981).

25. D. Ryu, T. W. Jones, and A. Frank, Numerical magnetohydrodynamics in astrophysics: Algorithm and tests for multidimensional flow, *Astrophys. J.* **452**, 785 (1995).

26. W. Shyy and S. S. Thakur, A controlled variation scheme in a sequential solver for recirculating flows. Part I. Theory and formulation, *Numer. Heat Transfer B* **25**, 245 (1994).

27. J. L. Steger and R. F. Warming, Flux vector splitting of the inviscid gas-dynamic equations with applications to finite difference methods, *J. Comput. Phys.* **40**, 263 (1981).

28. T. Tanaka, Finite volume TVD scheme on an unstructured grid system for three-dimensional MHD simulations of inhomogeneous systems including strong background potential field, *J. Comput. Phys.* **111**, 81 (1995).

29. T. Tang and K. Xu, Gas-kinetic schemes for the compressible Euler equations. I. Positivity-preserving analysis, *Z. Angew. Math. Phys.* **50**, 258 (1999).

30. B. van Leer, Towards the ultimate conservative difference scheme. V. A second-order sequel to Godunov's method, *J. Comput. Phys.* **32**, 101 (1979).

31. B. van Leer, *Flux-vector Splitting for the Euler Equations*, ICASE Report 82-30 (1982).

32. K. Xu, *Gas-kinetic Schemes for Compressible Flow Simulations*, 29th CFD Lecture Series 1998-03 (Von Karman Institute for Fluid Dynamics 1998).

33. K. Xu, *Gas-evolution Dynamics in Godunov-Type Schemes and Analysis of Numerical Shock Instability*, ICASE Report 99-6 (1999).

34. K. Xu, L. Martinelli, and A. Jameson, Gas-kinetic finite volume methods, flux-vector splitting and artificial diffusion, *J. Comput. Phys.* **120**, 48 (1995).

35. A. L. Zachary, A. Malagoli, and P. Colella, A higher-order Godunov method for multidimensional ideal magnetohydrodynamics, *SIAM J. Sci. Comput.* **15**, 263 (1994).